X-735-70-256
PREPRINT

NASA TM X- 63995

THE PHOTOCONDUCTIVE LAYER OF AVCS-APT VIDICON TUBES

JOHN J. PARK

JUNE 1970

GSFC
GODDARD SPACE FLIGHT CENTER
GREENBELT, MARYLAND

X-735-70-256

THE PHOTOCONDUCTIVE LAYER OF AVCS-APT VIDICON TUBES

John J. Park

June 1970

GODDARD SPACE FLIGHT CENTER
Greenbelt, Maryland

THE PHOTOCONDUCTIVE LAYER OF AVCS-APT VIDICON TUBES

John J. Park

SUMMARY

Analyses of the selenium and sulfur compositional variations in the photoconductive layers of typical vidicon tube face plates are presented. The thickness of the various layers and its variation with the manufacturer's optical measuring technique was determined. The presence of "grain boundaries" was noted in certain layers and this presence indicated a non-acceptable photoconductor. Electrical measurements of the photoconductive layers have shown the effect of compositional variation and of thickness variation, with the optimum thickness being on the order of 5000 - 6000Å.

CONTENTS

ILLUSTRATIONS

TABLES

THE PHOTOCONDUCTIVE LAYER OF AVCS-APT VIDICON TUBES

INTRODUCTION

A contract has been concluded with General Electrodynamics Corporation (GEC), Garland, Texas, for a study of the reproducibility of the photoconductive layer of GEC's vidicon tubes. These particular tubes have been used in the Automatic Picture Transmission (APT) system and in the Advanced Vidicon Camera System (AVCS), on the TOS-ESSA satellite.

The AVCS vidicon tube and the APT vidicon tube are identical, though the AVCS has a 6-1/2 sec. readout while the APT has a 200 sec. readout. In the selection process for the APT tubes from those purchased for AVCS use, a relatively high rejection rate was encountered due to loss of sensitivity and poor image storage capabilities. The Materials R&D Branch was requested to determine the reliability and reproducibility of the technique of preparing the active photosensitive layer on the quartz window.

The contract with GEC involved the production of a number of typical face plates, as would be prepared for the finished vidicon tube. The series of plates would be examined in a number of ways at GSFC and their uniformity determined. In addition other face plates were prepared with the thickness of the deposited layer being monitored by variations of GEC's usual technique. Also, some plates having flaws which would normally cause rejection would be analyzed in an attempt to determine the type of flaw or reasons for its occurrence.

The final report from GEC contained their measurements of thicknesses and their comments regarding variations in thickness, composition, techniques, and results. In preparing this Technical Note, portions of the GEC report are included, as indicated specifically or by quotation marks.

TECHNIQUES

The produced face plates, complete with the electroconductive layer and the vapor-deposited photoconductive layer, were subjected to various analytical techniques. Quantitative and qualitative analyses of the photoconductor were carried out by use of an electron microprobe. Reflectance and transmission patterns were obtained as a means of determining layer thicknesses and in comparing deposits. The thickness measurements by reflectance calculations were supplemented by measurements with an Angstrometer. In addition the optical metallograph was useful in noting differences in conductor appearance.

The electron microprobe uses an electron beam focused on the sample with the resultant x-ray fluorescence permitting qualitative analysis of the elements within the 1-micron diameter area. The characteristic x-rays also permit the estimation of the amount of material present. The electron beam is traversed slowly along a particular direction while the total x-ray pulses are counted; the analysis can be programmed to occur for a known time interval and the beam can be moved a known distance for an additional analysis.

The transmission and reflectance patterns were obtained over the region from 3400 millimicrons to below 500 millimicrons. The scanning spectrophotometer recorded the absorption bands in the transmission pattern and helped show the slight shifts in bands for the various samples; the intensity of the transmitted light was also dependent upon the quality of the photoconductive layer. The reflectance patterns showed that the photoconductor acted as an anti-reflecting film, yielding a uniform distribution of maxima and minima; the positions of the maxima and minima permitted the calculation of the thickness of the particular surface.

The Angstrometer uses phase contrast light with its resultant fringes for determining the thickness of a deposited layer. By vapor-depositing a layer, as of aluminum, across the edge or upon a scratch of the photoconductive layer, the fringe shift due to the change in plane at the scratch or edge permits a determination of the thickness. Because the fringes are 2945 Å apart the shift may be a fraction of one or more fringes and thus a layer's thickness may be estimated to within 100 Å.

Observations of the photoconductive surface could be made using the optical metallograph. The fineness of the deposited layer often made it difficult to focus upon the surface. The observations were usually done at 1000X. This technique was useful in detecting some interesting variations in surface appearance which could be correlated with the transmittance pattern.

SAMPLES AND SPECIMENS

The contractor prepared a large number of face plates in the normal vapor-deposited manner. These were called Phase I or Phase II plates. The face plates of Phase I were intended to be the typical or reference ones made in the contractor's normal manner. These of Phase I were six sets of six each and made a week or more apart so that there would be the normal personal and set-up variability. The Phase II plates consisted of 20 different sets of 3 each which were prepared for evaluation of the accuracy and sensitivity of the contractor's optical thickness monitoring system; these sets were prepared with white light and with red, green, or blue filters in the light path. Plates which exhibited

flaws, as pinholes, sufficient for rejection under the inspection procedure were also examined to determine the type or composition of the contaminant. Portions of the screen mesh were also submitted and examined for particles, contamination, or flaws in the mesh.

The contractor received the results of the various analyses at GSFC and also copies of the reflectance and transmission patterns. A final report of the contractor's results and conclusions were submitted to GSFC; there were no major differences of opinion regarding the results and certain comments from the contractor's report will be included, as indicated.

RESULTS

Phase I

Electron Probe Analysis of Set 1—Plates numbered 1 and 4 had been prepared with the numbers 1 to 12 deposited under the photoconductor, thus providing markers for analysis along the respective radii. Analyses for selenium and sulfur were made along the radius at five or more points, five microns apart and then again approximately 1000 microns closer to the center of the face plate; there were thus 8 analyses per radius. In this way, there were 96 different areas analyzed which permit a type of contour map of the deposited material.

The sulfur/selenium ratios were determined for the separate radii, from which the diametral analyses were calculated. As can be expected, the average for the radii, for the diameters, and for the circles do not all give the same results, as shown in Tables 1 and 2. However, these deposited layers are relatively uniform. There were certain extremes within a radius average, as, for example, in line 10 of plate #1 the high and low were 0.263 and 0.255 and the overall average was 0.259. Similarly one point in line 2 had a very low S/Se ratio of 0.222, due to a low total sulfur count. The normal counting rate was approximately 160 counts/sec for sulfur and 6,000 counts/sec for selenium. Tables 1 and 2 give the resultant averages for these plates 1 and 4 of Set 1, and Figure 1 presents the ratios in graphical form for plate 1.

Set 2—A few slight changes were made in analysis procedure for Set 2, as compared to the methods mentioned previously. At each area of analysis the sample was continuously moving at 96 microns/minute and the detectors collected counts for 20 seconds; at the end of the 20 seconds the sample was automatically stepped 5 microns further and then a second analysis was begun. Previously, the sample had been stationary for the 20 seconds of data collecting; some evaporation of the sample could have occurred under the impact and consequent heating by the electron beam, though no burn spot was observed. This sample had also

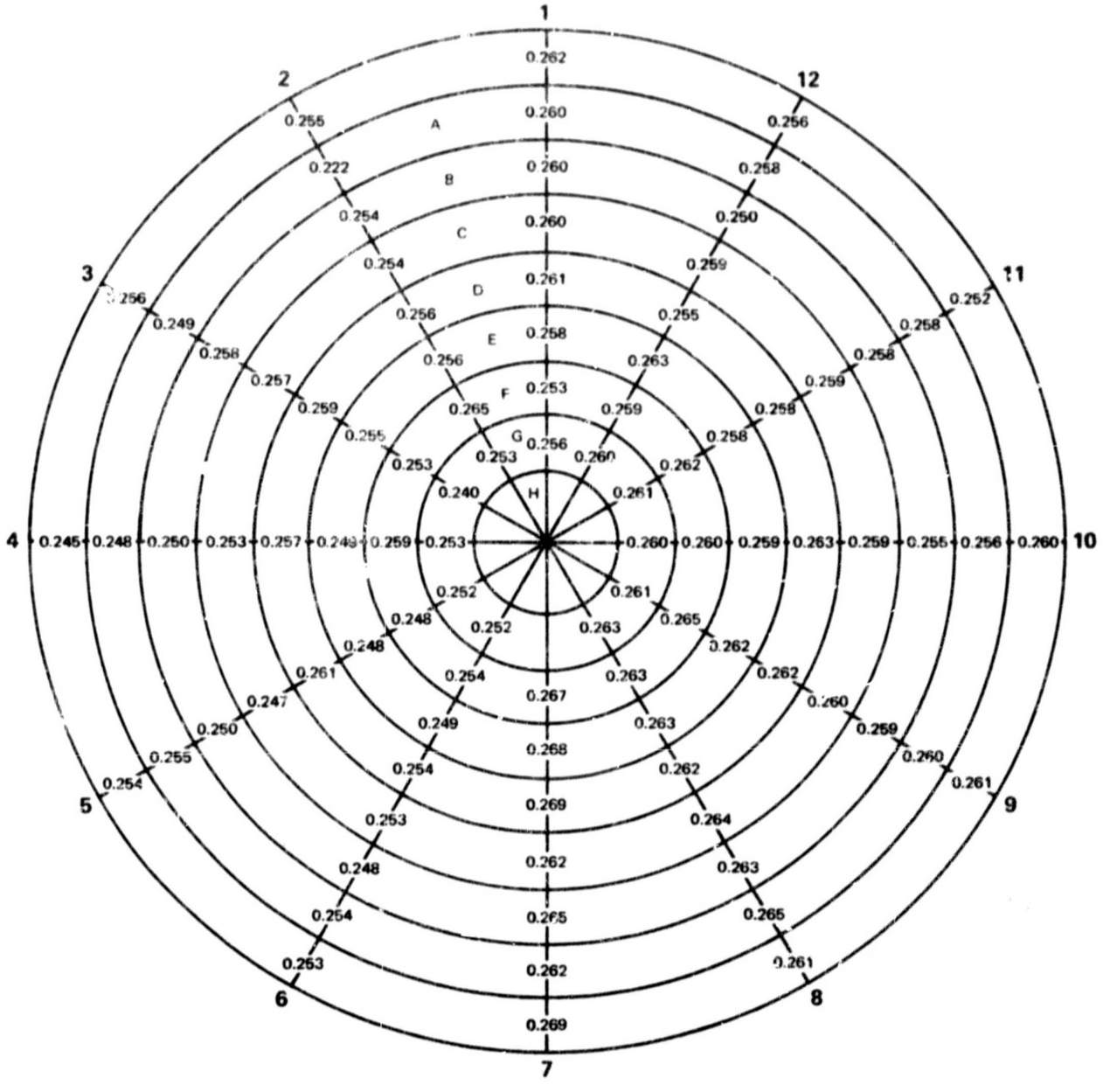

AVERAGE OF ALL POINTS: 0.25969
STANDARD DEVIATION: 0.00654
PERCENT STANDARD DEVIATION: 2.55

Figure 1. S/Se Count Ratios for Phase One, Set-1, Sample-1

Table 1

Probe Analyses for Plate 1, Set 1

Radius S/Se	Diameter S/Se	Circle S/Se
1 0.259	1 - 7 0.262	A 0.257
2 0.252	2 - 8 0.257	B 0.254
3 0.253	3 - 9 0.257	C 0.256
4 0.252	4 - 10 0.255	D 0.257
5 0.252	5 - 11 0.255	E 0.260
6 0.252	6 - 12 0.255	F 0.257
7 0.266		G 0.259
8 0.263		H 0.256
9 0.261		
10 0.259		
11 0.258		
12 0.258		

Average of all points	0.25969
Standard Deviation	0.00654
Percent Standard Deviation	2.55

Table 2

Probe Analyses for Plate 4, Set 1

Radius S/Se	Diameter S/Se	Circle S/Se
1 0.249	1 - 7 0.250	A 0.247
2 0.243	2 - 8 0.242	B 0.248
3 0.255	3 - 9 0.253	C 0.247
4 0.242	4 - 10 0.250	D 0.247
5 0.240	5 - 11 0.240	E 0.247
6 0.249	6 - 12 0.249	F 0.248
7 0.251		G 0.247
8 0.241		H* 0.248
9 0.251		
10 0.258		
11 0.240		
12 0.251		

*Circle H is average of 7 values

Average of all points	0.24728
Standard Deviation	0.00618
Percent Standard Deviation	2.49

been moved in 5 micron steps between analyses. Also, for Set 2 and subsequent sets the radii were analyzed in a random order rather than successively as in the prior set of analyses.

The results of the analyses of Plate 1 is given in Table 3 and for Plate 4 in Table 4. As indicated in the Tables, the average S/Se ratio for Plate 1 is 0.285, and the average S/Se ratio for Plate 4 is 0.279. The individual point analyses for Plate 1 range from a low of 0.269 to a high of 0.298 and for Plate 4 from a low of 0.268 to a high of 0.290.

Table 3

Probe Analyses for Plate 1, Set 2

Radius S/Se	Diameter S/Se	Circle S/Se
1 0.279	1 - 7 0.284	A 0.284
2 0.283	2 - 8 0.283	B 0.286
3 0.291	3 - 9 0.286	C 0.287
4 0.286	4 - 10 0.287	D 0.284
5 0.287	5 - 11 0.288	E 0.285
6 0.281	6 - 12 0.280	F 0.286
7 0.289		G 0.285
8 0.285		H 0.286
9 0.282		
10 0.289		
11 0.290		
12 0.279		

Average of all points 0.285
Standard Deviation 0.00575
Percent Standard Deviation 2.02%

Table 4

Probe Analyses for Plate 4, Set 2

Radius S/Se	Diameter S/Se	Circle S/Se
1 0.277	1 - 7 0.273	A 0.279
2 0.277	2 - 8 0.280	B 0.277
3 0.277	3 - 9 0.277	C 0.277
4 0.276	4 - 10 0.280	D 0.282
5 0.278	5 - 11 0.276	E 0.280
6 0.283	6 - 12 0.282	F 0.279
7 0.279		G 0.279
8 0.283		H 0.278
9 0.277		
10 0.283		
11 0.275		
12 0.281		

Average of all points 0.279
Standard Deviation 0.00475
Percent Standard Deviation 1.73%

Repeating the analysis and using the method in which the electron beam was stationary during the 20 seconds of analysis, the results for Plate 1 are different, having an average ratio of 0.256 for all points. The accumulated counts showed a greater variation than for the results mentioned above, and this scatter is believed due to some evaporation of the constituents.

Set 3—Plate 1 has a sulfur-to-selenium average ratio of 0.289 and Plate 4 has an average ratio of 0.267. The difference in the average analysis between these two plates is higher than for Set 2, being 0.022 as compared to a difference of 0.006 for the two analyses of Set 2 plates. The average analyses for Sets 2 and

3 are also higher than for Set 1, though the change to the moving electron beam may have contributed somewhat to obtaining a higher count rate on the last two sets.

Set 4—The sulfur/selenium ratio for Plate 1 is 0.326 and for Plate 4 is 0.304. The ratio of 0.326 is the highest obtained thus far for any of the Phase I plates and the ratio of 0.304 is also much higher than any previous results. The highest previous ratio was 0.289 and the lowest was 0.247. As may be noted in Figure 2, the separate ratios are all fairly consistent and uniform. There is no reason to suspect a variation in analytical techniques. Consequently, it was concluded that the deposited layers, though showing little compositional variation from point to point, have a significantly higher sulfur/selenium ratio.

Sets 5 and 6—The sulfur/selenium ratios for these two sets were significantly higher than any of the previous analyses. The average of all points for Plates 1 and 4 of Set 5 were 0.437 and 0.410, respectively, and for Plates 1 and 4 of Set 6 were 0.366 and 0.372, respectively. These results are compared with those for the other sets in Table 5, in which the difference in analyses is apparent. A noticeable increase in the ratio occurred with the last three sets. Prior to the delivery of Sets 4, 5, and 6, GEC reported that they were not making APTS tubes at the time Sets 4, 5, and 6 were made and that these sets were prepared specifically to fill the term of this contract.

Table 5

Sulfur/Selenium Ratios for Phase I Sets

	Plate 1	Plate 4	Average
Set 1*	0.259	0.247	0.253
Set 2	0.285	0.279	0.282
Set 3	0.289	0.267	0.278
Set 4	0.326	0.304	0.315
Set 5	0.437	0.410	0.423
Set 6	0.366	0.372	0.369

*Analyzed with stationary, rather than moving, electron beam.

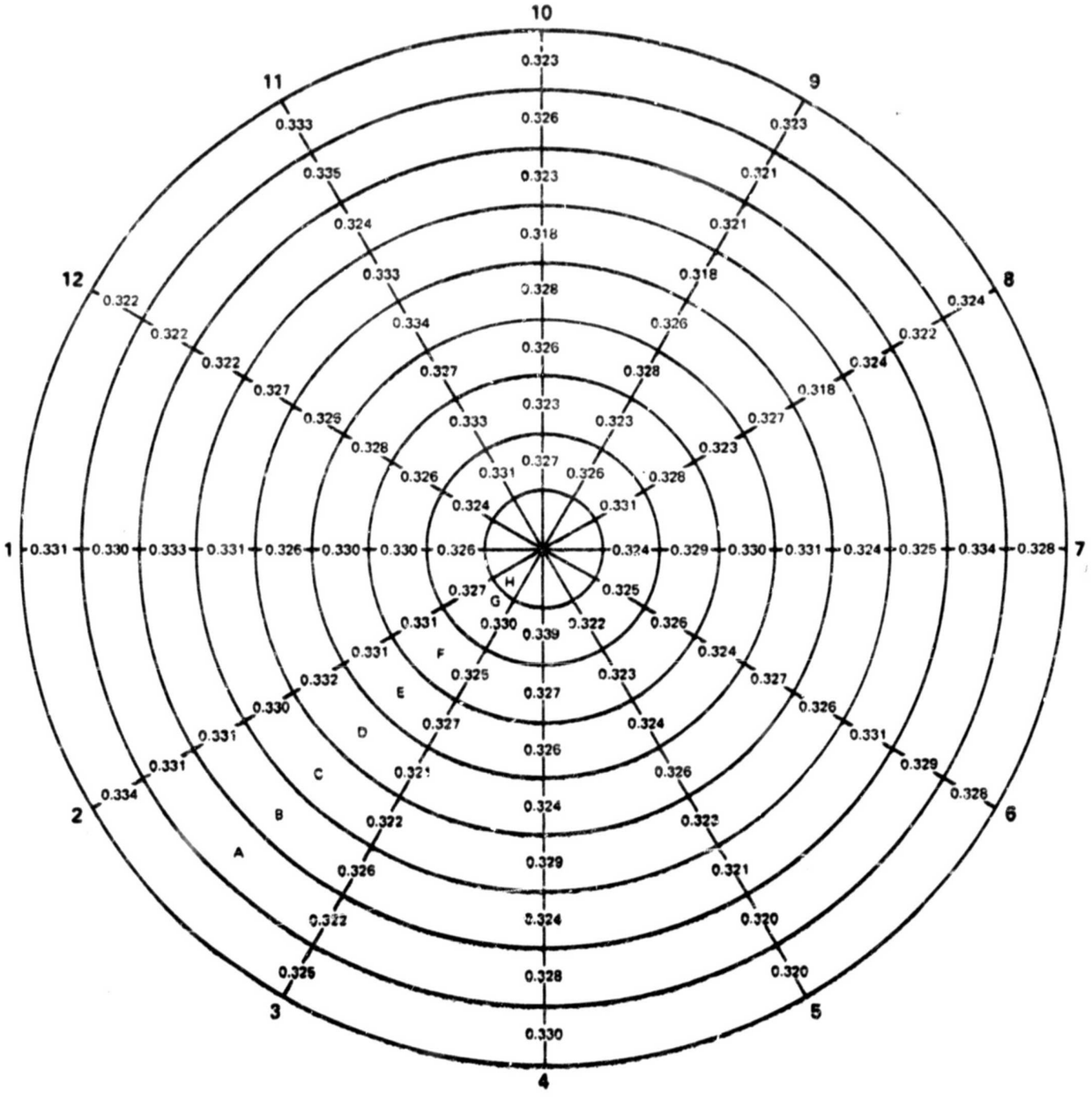

Figure 2. Phase 1, Set 4, Sample 1, S/Se Ratios

In a discussion of the results of the probe analyses, particularly with regard to the higher sulfur/selenium ratios of Sets 4, 5, and 6, it was learned that GEC had experienced a series of problems with the manufacture of other slow scan vidicons. Quoting the GEC report, those vidicons "showed very low sensitivity, very low dark current, and a stubborn refusal to show any change in sensitivity during the post-exhaust baking period." Their previous studies had indicated that the sulfur content was high, and after lowering the sulfur content of the starting material they were able to obtain tubes having the desired previous sensitivity, dark current, and thermal behavior. However, they were "unable to determine the original cause of the shift in the photoconductor composition." They were convinced, as were we, that the analyzed ratios were indicative of a change in the photoconductor composition.

Thickness Measurements of Set 1—The thicknesses of the deposited photoconductor for Plates 1, 3, 4 and 6 were determined by Angstrometer measurements. The thicknesses for Plates 2 and 5 were calculated from their reflectance patterns. A set of scratches were made on Plates 1, 3, 4 and 6 and their relationship to a red mark on the back of the plates were as shown in Figure 3. The red mark was described as being near the point of tangency to the "outer circle" in the deposition chamber at GEC.

The individual readings were made along certain edges or scratches made in the photoconductor (Figure 3), and the results are as shown. In Plate 1, for example, the average of the four measurements is about 6900 Å with a spread of 850 Å between the high and low measurements; the area of thinnest photoconductor is apparently in the region where the red mark had been made. The summary of the thickness measurements is as follows:

Plate	No. of Measurements	Thickness Å	Technique
1	4	6900	Angstrometer
2	1	6450	Reflectance
3	2	6580	Angstrometer
4	4	6270	Angstrometer
5	1	6520	Reflectance
6	2	7010	Angstrometer

The thickness as calculated from the reflectance pattern compares very well with the results as determined with the Angstrometer.

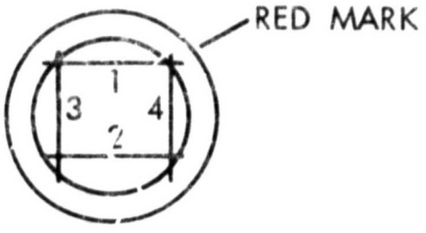

POSITION 1 - 6520Å
2 - 7370
3 - 7060
4 - 6660

PLATE 1, SCRATCHES 1, 2, 3, 4 ON CIRCULAR PHOTOCONDUCTOR

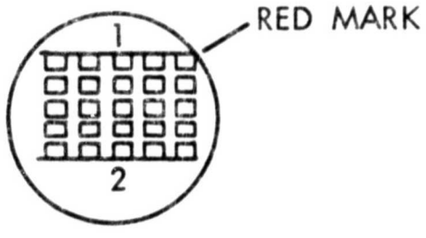

POSITION 1 - 6330Å
2 - 6830

PLATE 3, MEASUREMENTS 1 AND 2 AT EDGE OF SQUARE ARRAY

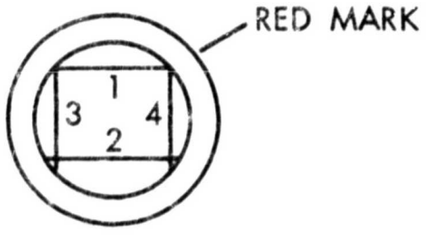

POSITION 1 - 5890Å
2 - 6320
3 - 6665
4 - 6210

PLATE 4, SCRATCHES 1, 2, 3, 4 ON CIRCULAR PHOTOCONDUCTOR

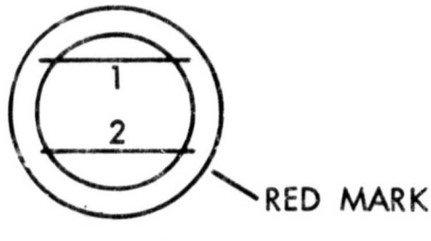

POSITION 1 - 6710Å
2 - 7310

PLATE 6, SCRATCHES 1, 2 ON CIRCULAR PHOTOCONDUCTOR

Figure 3. Location of Area for Angstrometer Measurements, Phase I, Set 1

Thickness of Set 2—The reflectance patterns were used in calculating the thickness of the photoconductor. The results of the calculations are as follows:

Photoconductor Thickness	
Plate 1	8300 Å
Plate 2	8240 A
Plate 4	8000 A
Plate 5	7960 A
Plate 6	8020 A

The average of these calculations is 8104 Å, which is approximately 1580 Å thicker than the average of the Set 1 thicknesses.

Thickness of Set 3—The calculations of the photoconductor thickness were made from the measurements of the reflectance patterns. One Angstrometer measurement was made for confirmation. The results of the calculations are as follows:

Photoconductor Thickness	
Plate 1	6490 Å
Plate 2	5860 A
Plate 3	5675 A (by Angstrometer)
Plate 4	5410 A
Plate 5	6000 A
Plate 6	6340 A

These values show relatively poor uniformity with an average value of 5962 Å and a spread of 1080 Å. For comparison, the average thickness for the Set 1 plates was 6621 Å and for Set 2 plates was 8104 Å.

Thickness of Set 4—The reflectance patterns were also relatively uniform for the samples of this set. The results from these calculations are as follows:

Thickness of Photoconductive Layer Phase I, Set 4 Face Plates	
Plate 1	5930 Å
Plate 2	6030 A
Plate 4	6470 A
Plate 5	6600 A
Plate 6	7260 A

As may be noted, the thicknesses increase with the number of the plate, which is presumably the order of manufacture. This would imply a gradual increase in the deposition time. None of the other sets showed a progressively thicker layer, the thicknesses varying randomly. The average for these five plates is 6458 Å, which is reasonably close to the average for Sets 1 and 3.

Thickness of Set 5 and Set 6—As may be noted, the average thickness of the Set 5 plates is 7165 Å and of the Set 6 plates is 5966 Å. The spread for the Set 5 plates is 1530 Å, while the spread for the Set 6 plates is 850 Å.

Thickness of Deposited Layers

A. Phase I, Set 5

Sample	1	7880 Å
	2	7380
	3	6910
	4	6660
	5	6350
	6	7810
Average		7165

B. Phase I, Set 6

Sample	1	5550 Å
	2	6310
	3	5670
	4	5910
	5	5960
	6	6400
Average		5966

Metallographic Observations

In preparing the face plates of Set 2 for electron probe analysis, it had been noticed that the appearance of the photoconductor surface was relatively rough. For the Set 1 it had been difficult to focus visually on the surface because of its obvious smoothness and uniformity. This difference in appearance at 1000X is shown in Figure 4, with the larger "grains" being for the Set 2 face plates, as compared with a Set 1 face plate.

In the scanning electron microscope, the higher magnification and the greater depth of field show the unusual appearance of the Set 2 plates. At 8500X, see Figure 4D, it is apparent that the photoconductor is "spongy" appearing or is separated into relatively large discrete areas.

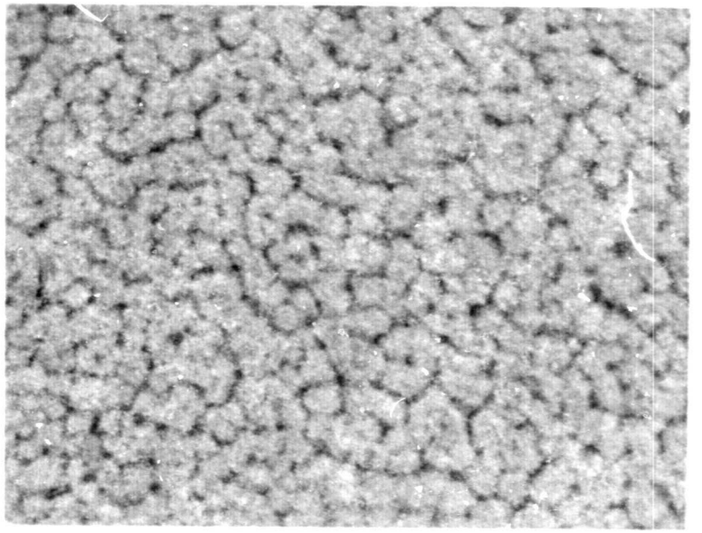

A. Set 2, Plate 1 x 1000

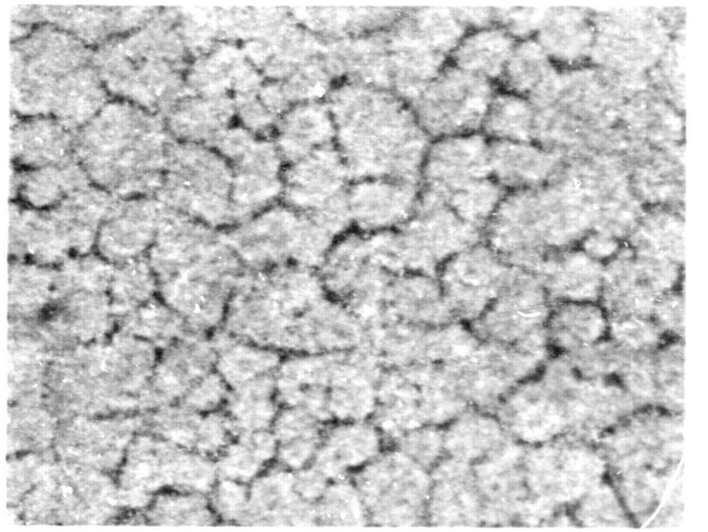

B. Set 2, Plate 2 x 1000

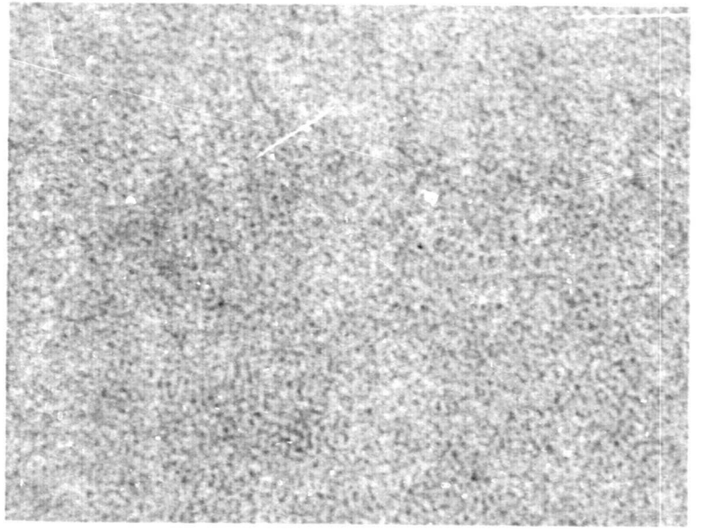

C. Set 1, Plate 5 x 1000

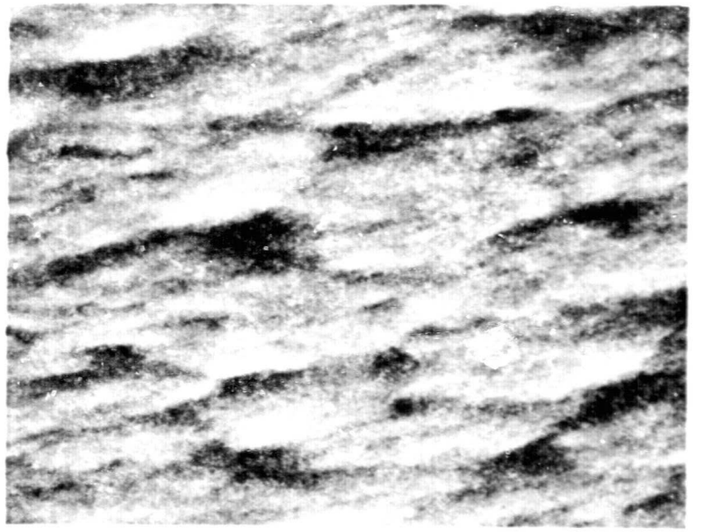

D. Set 2, Plate 1, Scanning Electron Microscope Picture X8500

Figure 4. Photoconductive Surface as Observed at High Magnification

An estimate of the apparent size of the "grains" in face plates 1 and 2 of Figure 4 was made. Using the micrograph of a scale at the same magnification, the diameter of the "grains" in Plate 1, Figure 4A, is about 0.004 mm and in Plate 2, Figure 4B, is about 0.008 mm. For Plate 5 of Set 1, Figure 4C, the diameter is obviously very small, being perhaps 0.0001 mm, though it is very difficult to estimate.

For the Phase I Set 6 plates, one particular anomaly was observed: Plate 3 had a variety of grains. The Plate 3 is deposited as 25 squares in a 5x5 array. After examination of these squares, the following "grain sizes" of the middle and of the corner squares were noted:

	medium	small
	tiny	
tiny		small

Unfortunately no orientation mark had been made on the back of this plate so that a relationship to the manufacturing lay-out could be made. This is the first time that a variation in grain size within a single plate had been observed.

Transmittance Patterns of Set 1

The patterns for a number of plates were obtained for the wavelength range of 3400 to 190 millimicrons on a Beckman DK-1A Recording Spectrophotometer. It was observed that the transmission was reduced at various wavelength regions and that there was complete absorption below about 550 millimicrons. The pattern for Plate 2 of Set 1, which had a photoconductor thickness of 6450 Å, is presented in Figure 5; most of the patterns were similar. However, a few of the patterns showed a relatively high absorption, as for Plate 1 of Set 2 (Figure 6). This particular face plate had medium size "grains" which undoubtedly contributed to the total absorption by internal reflections. It was later determined after comparing the transmission pattern with the metallographic appearance that the presence of grains resulted in a poorer transmission pattern. It was also observed that the transmission only at 700 millimicrons would be a clue as to the presence of grains; the transmittance for the fine-grained Plate 2 Set 1 (Figure 5) is approximately 40% at 700 millimicrons while it is only 5% for the Plate 1 Set 2 (Figure 6) sample.

Discussion of Phase I Face Plates (from GEC Report)

Photoconductor Composition—"The unexpected results which were shown by these analyses involved the apparently sizeable increase in the sulfur content of

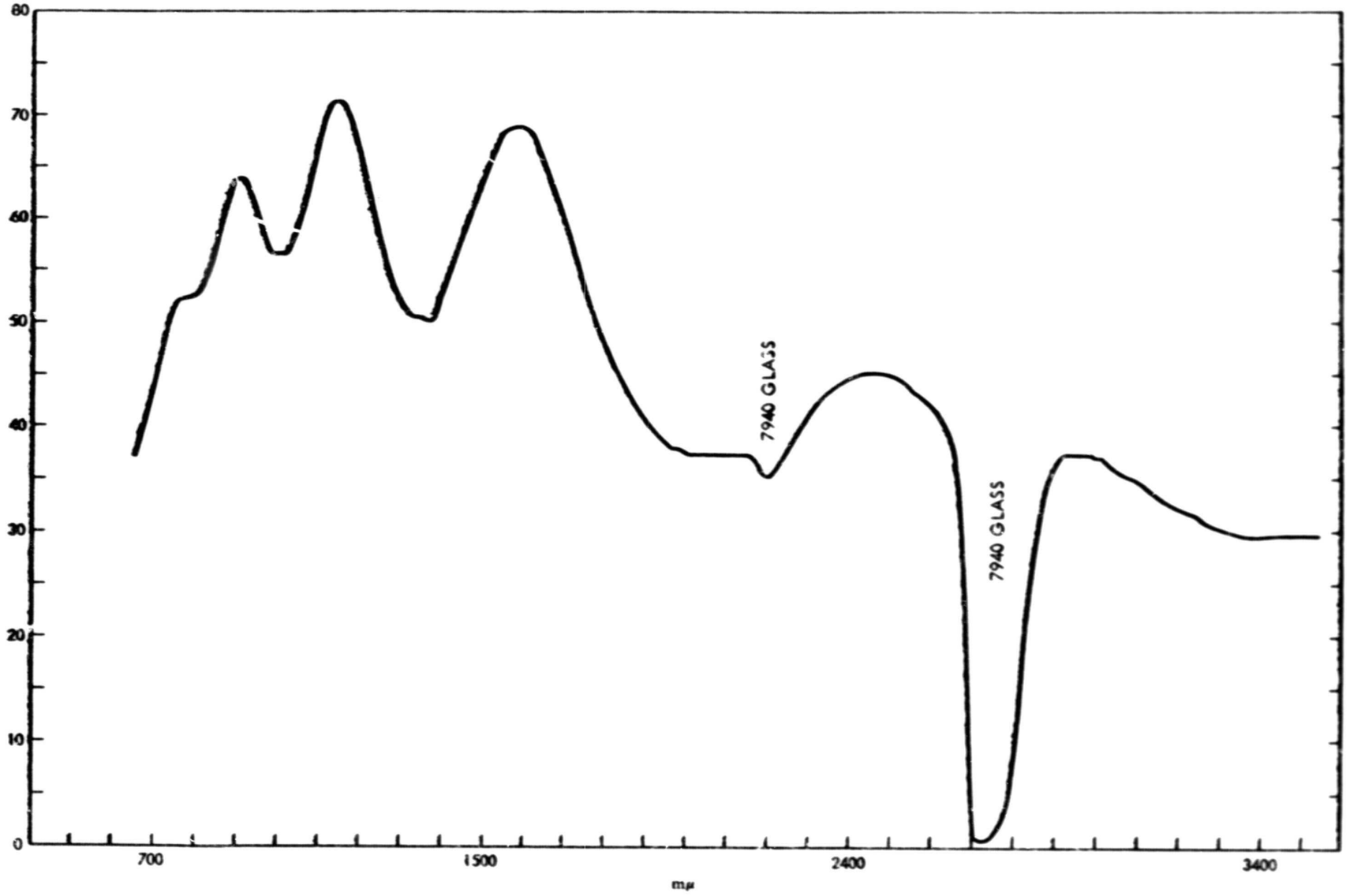

Figure 5. Transmittance Phase I, Set 1, Plate 2

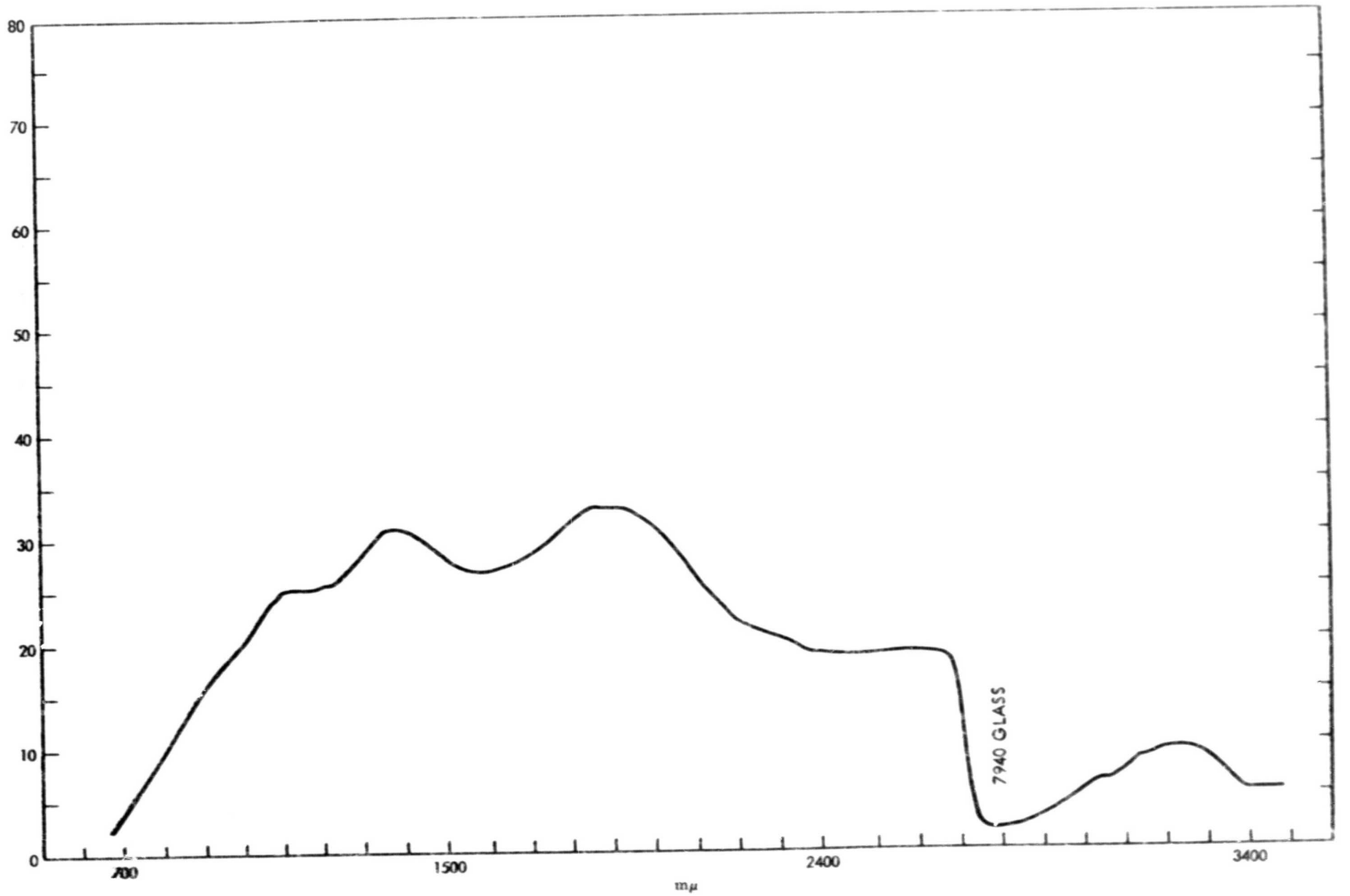

Figure 6. Transmittance Phase I, Set 2, Plate 1

face plates which were prepared before and after July, 1968. It would appear that there is a difference of some thirty percent or more in the sulfur content of face plates prepared for Set 3 and those prepared for Set 5. The increase in count ratio which was discovered at GSFC corresponds to a fairly sudden change in the properties of newly prepared slow scan vidicons which were prepared at GEC at the same time. Although it has been possible to correct the vidicon difficulties by changing the composition of the starting materials, no really satisfactory explanation has been discovered at GEC for the cause of the change in behavior of the older starting compositions.

Photoconductor Grain Size—The discovery of some very coarse grained photoconductor materials on some face plates which were investigated by GSFC is another unexpected result of this study.

At this point, a brief review of our empirically derived theory of the crystallograph of this photosurface is in order. The preparation of many Se/S photosurfaces here has led us to the conclusion that the photolayer, when it is initially deposited, is amorphous and glassy. Subsequent heat treatment of the photolayer causes a portion of the material to convert to the metallic hexagonal form. As has been long known even, or especially, to the very first people who built vidicons, selenium will remain in amorphous form at temperatures somewhat above its conversion point, if and only if there is no flaw, contamination, or tiny particle of material on the substrate. At the place where such a flaw or nucleation center does exist, an amorphous selenium layer very rapidly converts to the metallic, conductive form.

Examination of many experimental efforts has led us to believe that the GEC photosurface is a two phase system. There appears to exist an amorphous matrix which probably is very rich in sulfur. Trapped in this matrix, there appear to be very tiny crystallites of hexagonal type selenium. The presence of these crystallites is probably the explanation for GSFC's discovery some time ago of an identifiable hexagonal selenium x-ray diffraction pattern in the face plates of APTS vidicons. It appears to us that the function of the sulfur rich matrix is to provide an "unconvertible" barrier of photoconductive material which restricts the grain growth of the hexagonal selenium.

As we said above, the growth of hexagonal selenium from an amorphous layer of selenium is triggered by the presence of a nucleation center on the glass substrate. In the case of the forced conversion of the slow scan vidicon face plate the granular surface of the tin-oxide or NESA signal electrode provides a multitude of nucleation centers for the selenium material.

Returning to the results of photomicrographic studies of the thirty-six face plates of Phase One—our examination of the photographs of these surfaces leads us to the conclusion that the coarseness of grain is not caused by an overgrowth of the hexagonal selenium crystallites but by a deterioration of the matrix material. The major problem which arises in the evaluation of the microscopic data is that the slow scan photosurface is not stable in air for long periods of time. It is quite common for vidicon face plates to be rejected during inspection and left in the reject containers for several days before the glass is returned for salvage. Examination of face plates which have been held in this way for a few days generally reveal a change of color in the photolayer as well as a tendency of the photosurface to peel away from the glass substrate. Although the face plates which were shipped to GSFC were accorded more protection during storage than are the face plates in our reject bins, the effects of storage in atmosphere may very well account for the granularity of some of the face plates.

It is of course possible to develop several other explanations for the granular appearance of some of the face plates.

It is an obvious possibility that the rate of photoconductive deposition can have an effect on the surface grain. A review of the deposition data, however, shows no correlation between the deposition time for a given set of face plates and the appearance of granularity in the samples.

Another possible explanation is that the tin oxide signal electrode was in some way contaminated before the deposition of the photolayer. The presence of a layer of foreign material on the glass surface could cause rather large changes in the structure of the deposited layer.

A review of these and other possibilities leaves us without a firm explanation for the occasional appearance of a granular face plate. At this time, we are inclined to favor the storage-deterioration theory, but further work by GSFC on the relation of the photosurface structure to the underlying structure of the NESA coating may alter this opinion." (Above from GEC Report)

Phase II Face Plates

Sets 1-5—These Phase II face plates were obtained for examination concerning the accuracy of the optical thickness system used at GEC. The photoconductor thickness of all the face plates was determined by calculation from reflectance patterns, and Angstrometer measurements of selected photoconductor thicknesses were made for confirmation. Transmittance patterns were also obtained of at least one of each set. Micrographic observation of all face plates was also done.

These face plates were divided and labeled by GEC personnel into five parts which were called Sets 1 through 5 and were also rated as "23%T," "26%T," etc. The results of the thickness measurements and calculations rest upon the accuracy of determining the peak of the reflections; consequently, additional calculations were made using the maximum expected variation in determining the peak midpoint. These calculations showed that a difference of ±10 millimicrons from reflectance measurements result in a thickness difference of ±160 Angstroms. These particular face plates were made by GEC personnel using the normal white light in their system for thickness cut-off decisions.

In GEC's process, the optical monitor is operated during deposition by adjusting the intensity of the monitor light source until the monitoring photocell output current reads full scale on a microammeter. The face plates are then shielded, the Se/S material is heated to evaporating temperature and the shield is removed, and deposition begun.

These Sets 1-5 were prepared with white light, i.e., no filter, and they showed considerable variation in thickness. The greatest difference between thicknesses is for the three of "Set 5-32%," having a range from 3450 to 6350 Å. Also, the fact that the three of "Set 1-20%T" have an average thickness of 7323 A and the three of "Set 2-23%T" have an average thickness of 7493 Å is inconsistent with the apparent trend of thinner photoconductor layers with the indicated percentage.

The summary of all thickness results is given in Table 6.

Sets 6-10—In this series of depositions a red filter was used in the optical system; a range of indicated percent transmissions, from 60 to 74 "%T," were obtained for various thicknesses. Three samples in each set were received and analyzed.

Calculations of the deposited thickness were made from an analysis of the reflectance patterns of each of these fifteen face plates. It was obvious from looking at the reflectance patterns that differences in thicknesses between the three face plates of one set would be found. The calculations of thickness involve the number of fringes within a wavelength range and the wavelengths of the first and last fringes.

The calculated thicknesses show that there is a wide variation in thickness for the three plates of a set. For example, in Set 6, the thicknesses range from 11,260 Å to 8,290 Å. In addition, there is a discrepancy between Sets 6 and 7, for Set 6 with 60%T has an average thickness of 9393 Å while Set 7 with 64%T has an average thickness of 9673 Å.

Table 6
Review of Data from Phase Two Face Plates

Set	Sample	% Trans.	Filter	Thickness (A) Angstrometer	Thickness (A) Reflectance		
					GSFC	GEC	Grain
1	1	20	None	8120	7670	7830	Tiny
	2	20			6930	7730	Tiny
	3	20			7370	7200	Tiny
2	1	23	None		7380	7580	Tiny
	2	23		8215	7620	7720	Tiny
	3	23			7490	7630	Tiny
3	1	26	None		6150	6290	Tiny
	2	26			6830	6880	Tiny
	3	26		5280	5400	5340	Tiny
4	1	29	None		5680	5630	Tiny
	2	29		4445	4320	4540	Tiny
	3	29			5560	5780	Tiny
5	1	32	None		3450	3760	Small
	2	32		3600	4240	4220	Medium
	3	32			6350	4980	Large
6	1	60	Red		11260	8520	Tiny
	2	60			8290	11420	Tiny
	3	60			8630	8880	Tiny
7	1	64	Red		11920	12090	Large
	2	64			9500	9590	Tiny
	3	64			7600	7720	Tiny
8	1	68	Red		7350	7530	Tiny
	2	68			8530	8520	Large
	3	68			8400	8380	Tiny
9	1	72	Red		7430	7450	Tiny
	2	72			8280	8380	Tiny
	3	72			6760	6890	Tiny

Table 6 (Continued)

Set	Sample	% Trans.	Filter	Thickness (A) Angstrometer	Thickness (A) Reflectance		
					GSFC	GEC	Grain
10	1	74	Red		5120	5180	Tiny
	2	74			4510	4720	Tiny
	3	74			2650	2980	Tiny
11	1	18	Green		11870	11790	Large
	2	18			11400	11460	Large
	3	18			10330	10270	Large
12	1	21	Green		7000	6850	Large
	2	21			9430	9460	Tiny
	3	21			8790	8630	Tiny
13	1	24	Green		6600	6600	Tiny
	2	24			5870	6040	Tiny
	3	24			6560	6600	Tiny
14	1	27	Green		6120	6010	Large
	2	27			6060	6290	Tiny
	3	27			6420	6450	Tiny
15	1	30	Green		7290	7110	Large
	2	30			4810	4840	Large
	3	30			7290	7340	Tiny
16	1	3	Blue		8310	8140	Tiny
	2	3			7210	7150	Tiny
	3	3			8600	8450	Tiny
17	1	4	Blue		7010	7020	Tiny
	2	4			7100	7220	Tiny
	3	4			7430	7600	Tiny
18	1	5	Blue		6490	6230	Large
	2	5			6280	6460	Tiny
	3	5			6900	6700	Large

Table 6 (Continued)

Set	Sample	% Trans.	Filter	Thickness (A) Angstrometer	Thickness (A) Reflectance		
					GSFC	GEC	Grain
19	1	6	Blue		5560	5930	Tiny
	2	6			4960	5420	Tiny
	3	6			6450	6480	Large
20	1	7	Blue		4460	4390	Tiny
	2	7			4780	5250	Tiny
	3	7			4730	4990	Tiny

These results, though indicating poor control of the photoconductor thickness, are similar to the results reported above. In both instances there was a relatively wide range of thicknesses and there was an apparent discrepancy between indicated transmission of the optical system and the resultant average thickness of the deposited layers.

Sets 11-20—These specimens were prepared by using a filter in the light path, with Sets 11-15 made using a green filter and Sets 16-20 made using a blue filter. There are three specimens per set, each set having a specific transmission as determined with GEC's optical system and gage.

The thickness in Sets 11-15 range from 11,870 Å to 4,810 Å, though there is significant variation between the three plates for a set. Set 14 is the most uniform having a spread of only 360 Å for the three samples. The results are given in Table 6.

Sets 16-20, made with the blue filter, are generally very uniform in thickness. Too, the thicknesses show the proper trend, percent T increasing as the deposited layer becomes thinner, and there are no sets which are not in the expected order. Set 20 has a spread of 320 Å between the thickest and thinnest, and Set 17 has a spread of 420 Å. The results for the sets using the blue filter are the most consistent for any of the techniques used.

The resultant data for all sets are also graphed, using the individual points and averages for the three results. These graphs, Figures 7 to 10, show more obviously the wide spread within Sets and the non-linear change with %T. Only for samples made with the blue filter is there a reduced spread and a reasonable variation in thickness.

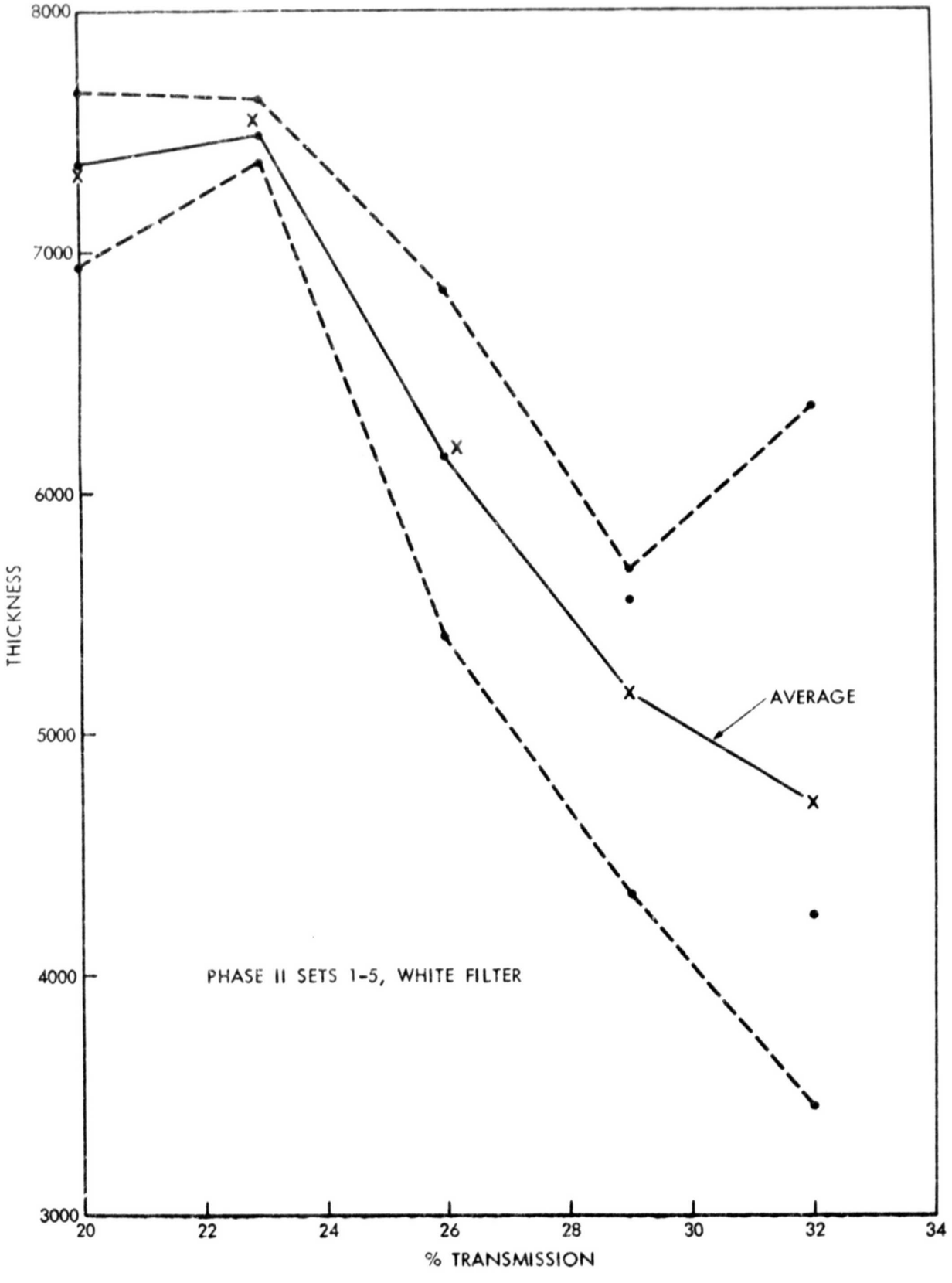

Figure 7. Thickness vs Percent Transmission, White Filter

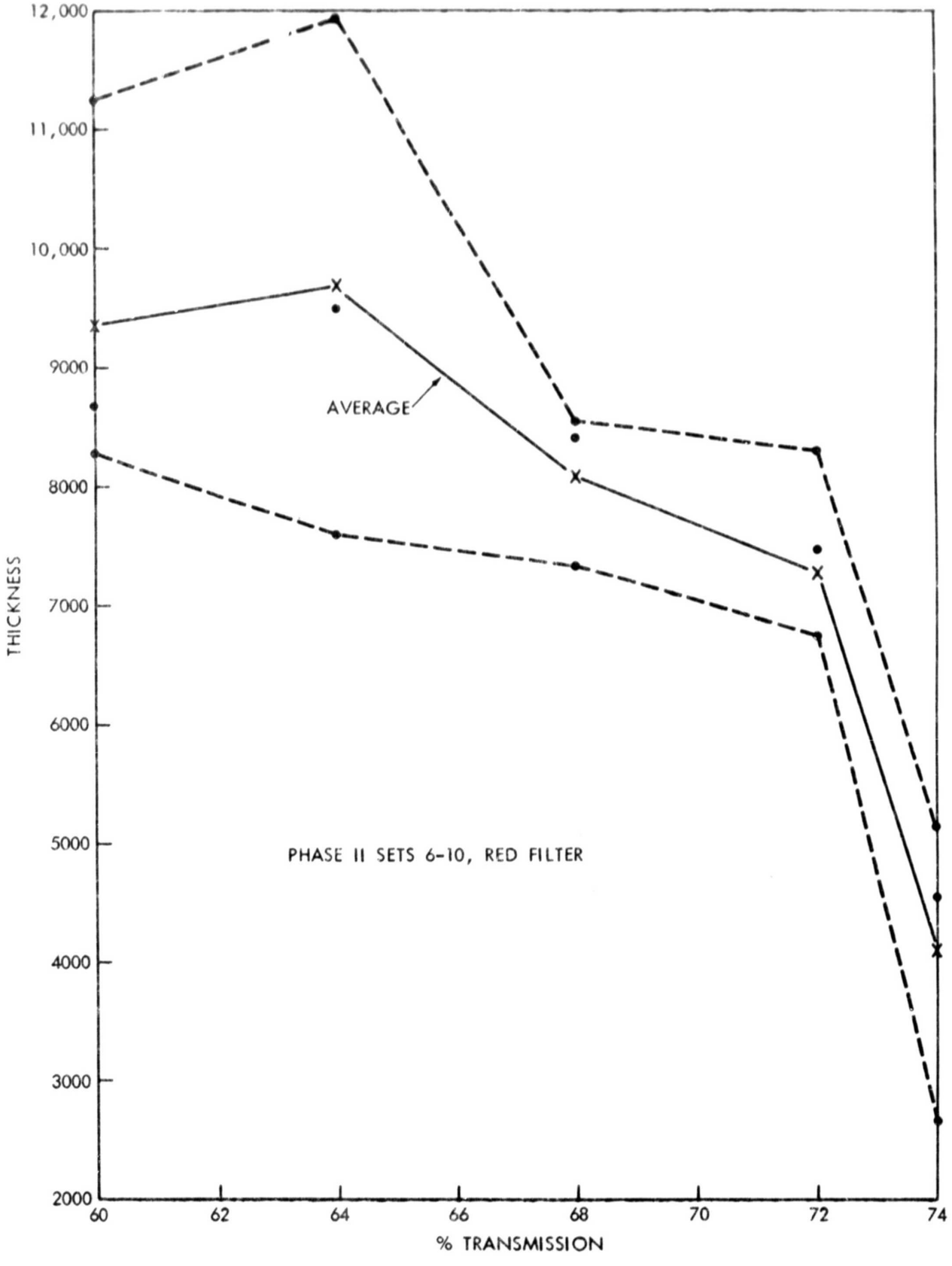

Figure 8. Thickness vs Percent Transmission, Red Filter

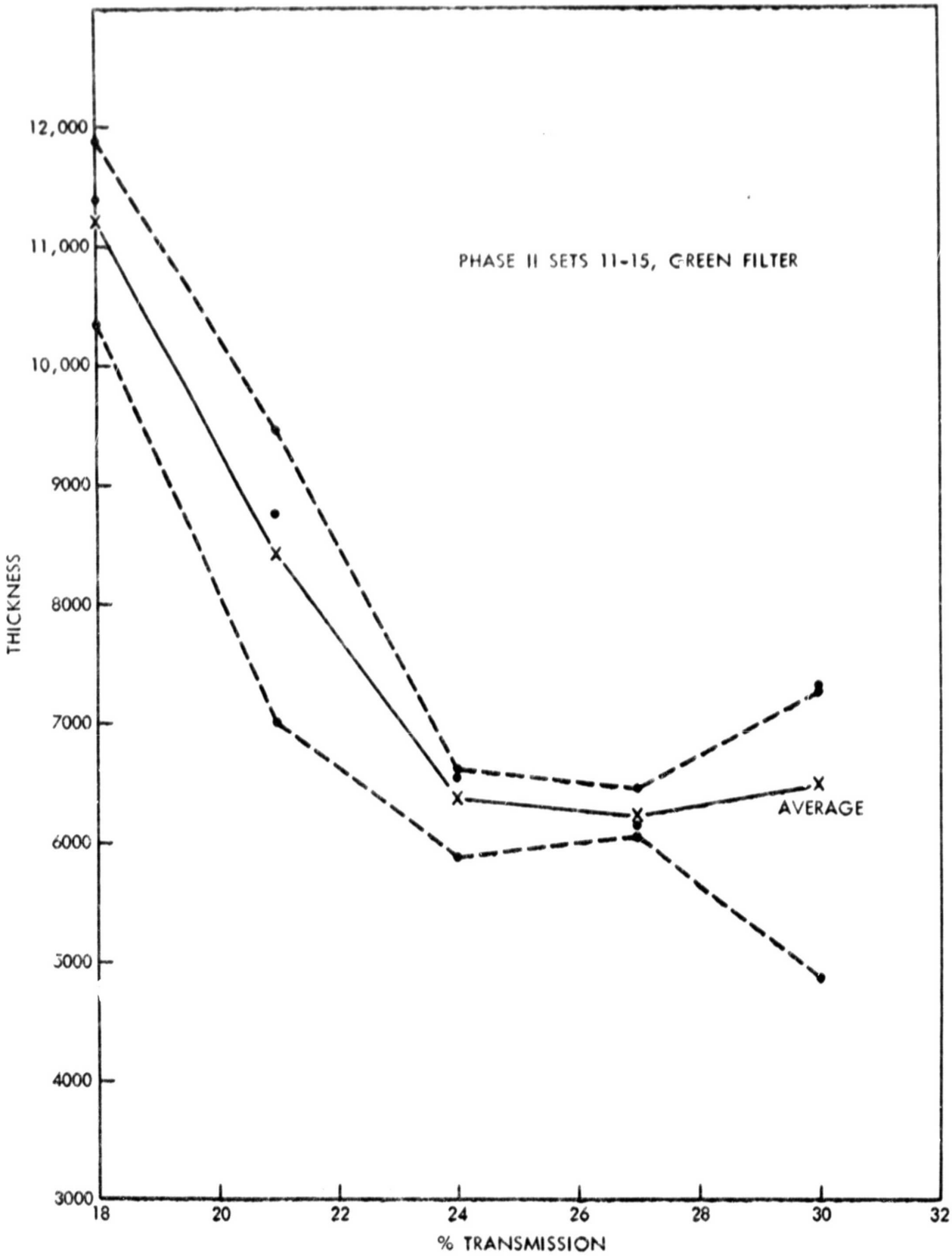

Figure 9. Thickness vs Percent Transmission, Green Filter

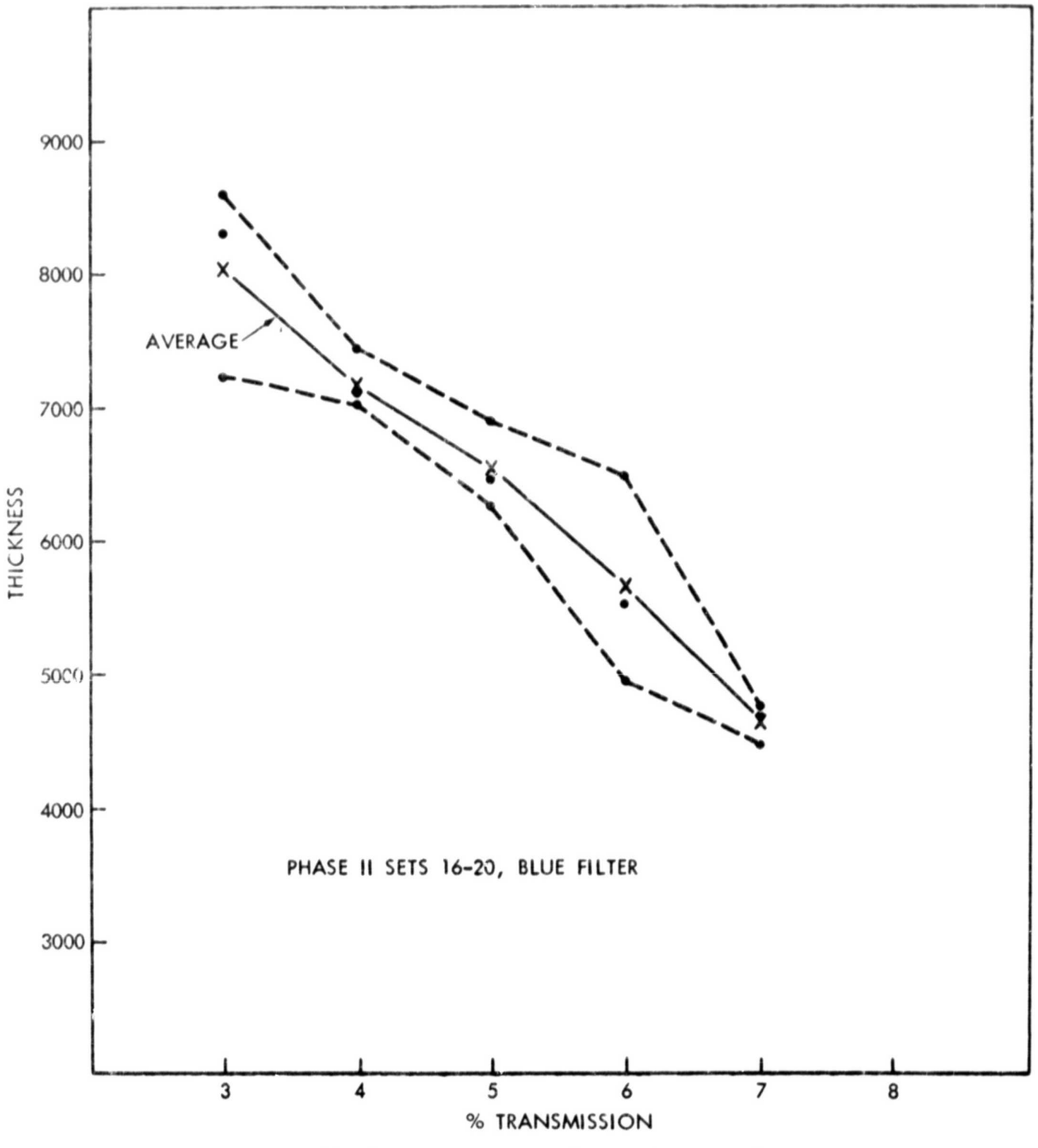

Figure 10. Thickness vs Percent Transmission, Blue Filter

The results were overwhelming; as GEC says, "The results of calculations from reflectance patterns and the results from the Angstrometer measurements indicate that the optical monitoring system which is used to control the thickness of the slow scan vidicon face plates is not as accurate as had been believed.

There is ample evidence that the thickness of the photosurface does vary in an uncontrolled manner from face plate lot to face plate lot."

One possible reason for the variation within the three samples of a set was the drift in the zero and 100% points used by GEC. This was suggested by GEC, since a few % change in the microammeter or in the photocell could result in an error in the thickness measurement.

Metallographic Observations

Under normal conditions, the observation of the photoconductor surface at 1000X was not easy, due to the difficulty of focusing on such a smooth surface. However, once it was noted that there were differences in appearance the observations became more than a routine operation. A number of surfaces had what were called "grains," the appearance being similar to an etched metallographic sample with grain boundaries.

The variation, as in Figure 11, was evident within the samples of a set, though there was not usually a gradation of "tiny" grains to "large" grains in going from Plates 1 to 3 of a set. Set 7-Sample 1 and Set 8-Sample 2 had different appearances, as shown in Figure 11, in which the contrast with another face plate of the same set is also shown. The reasons for the different surfaces are probably related to manufacturing procedures.

Examination of all of the photoconductor surfaces was also conducted for Sets 11-20. In a number of instances, the roughened, grainy appearance was noted, as mentioned in the previous statements. The samples having larger "grains" were:

Set 11, Samples 1 and 3
Set 12, Sample 1
Set 14, Sample 1
Set 15, Samples 1 and 2
Set 18, Samples 1 and 3
Set 19, Sample 3

The samples not listed had relatively smooth surfaces with very tiny "grains."

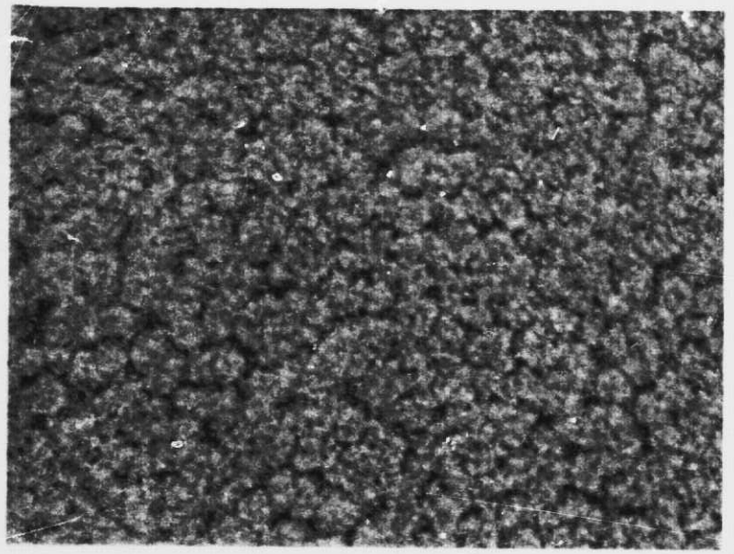

A. Set 7, Sample 1

B. Set 7, Sample 2

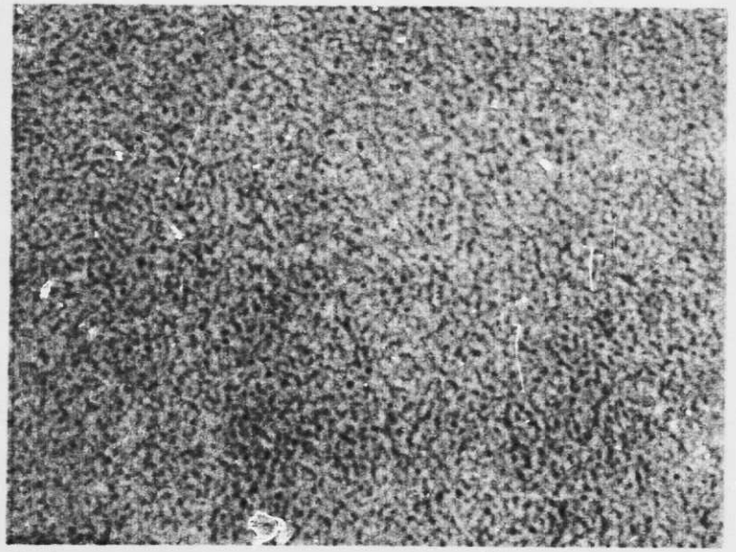

C. Set 8, Sample 1

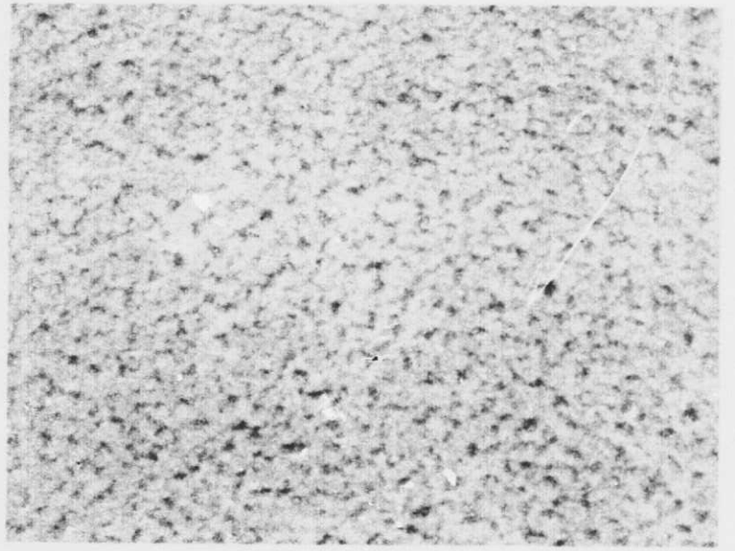

D. Set 8, Sample 2

Figure 11. Appearance of Photoconductor Surface. Reflected Light, 1000 X

The occurrence of the grains is puzzling, particularly as in Set 11 where only Sample 2 has the tiny grains while Samples 1 and 3 have obvious grains. Presumably, any three face plates of one set were made in succession with an insignificant time lapse between the three depositions. It is highly possible that variations in deposition technique cause the resultant variations in photoconductor surface appearance.

The use of the scanning electron microscope also verified that there was "depth" to the grain boundaries, Figure 12. The possibility of substrate roughness was suggested by GEC as related to the appearance of grains. The replication of the Nesa-coated quartz and of the photoconductor did not show any such correlation. The Nesa-surface was replicated after removal of the photoconductor by dissolution (Figure 12).

It was also noted that the reflectance and transmittance patterns indicated when a surface with large grains was being tested. The appearance of the larger "grains" coincides with a reflectance pattern having relatively lower peak-to-peak heights and with a transmittance pattern also being relatively "smooth" with less obvious transmittance windows. There is also a noticeable shift in the location of the transmittance and adsorptance "peaks" with the differences in photoconductor thickness.

As GEC commented, "The most important point which has been discovered with this set of face plates is the large granularity of the photosurface. GEC and GSFC personnel have discussed possible causes of this particular condition and have arrived at a list which includes:

a. Substrate temperature
b. Deposition rate
c. Texture of the SnO_2 signal electrode
d. Temperature of the evaporating material
e. The atmosphere in the evaporator
f. Post deposition shock
g. Exposure to moisture over extended periods of time

The results obtained from granular faced vidicons have not been evaluated but one possibility arises. It is not uncommon for slow scan vidicons during the first few hours of their holding period to develop very high dark currents. This has always been attributed to "over conversion" of the hexagonal selenium phase. That is, it has been thought that so much of the surface changed to the hexagonal conductive state, that the remaining amorphous matrix was unable to stand off the applied target voltage. It is entirely possible that the development of high dark current is the result of the physical aggregation of the photosurface which allows the passage of beam current through the interstitial spaces."

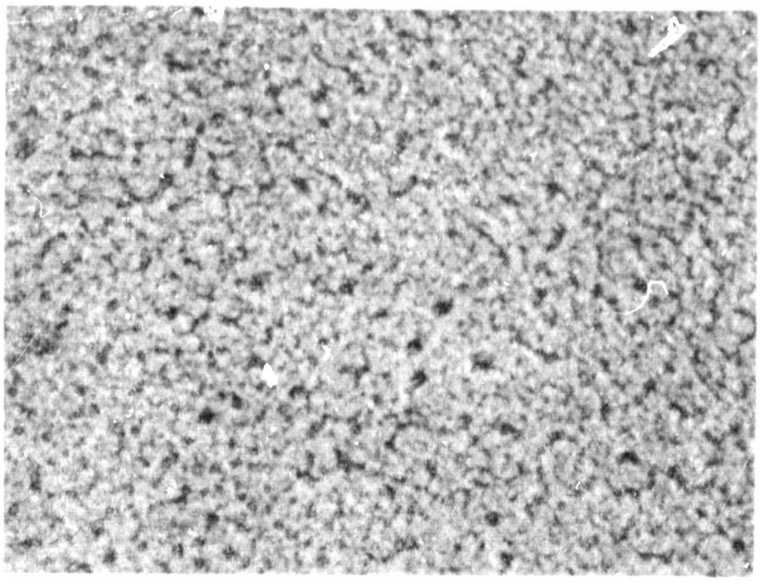

A. Optical Microscope, X1000

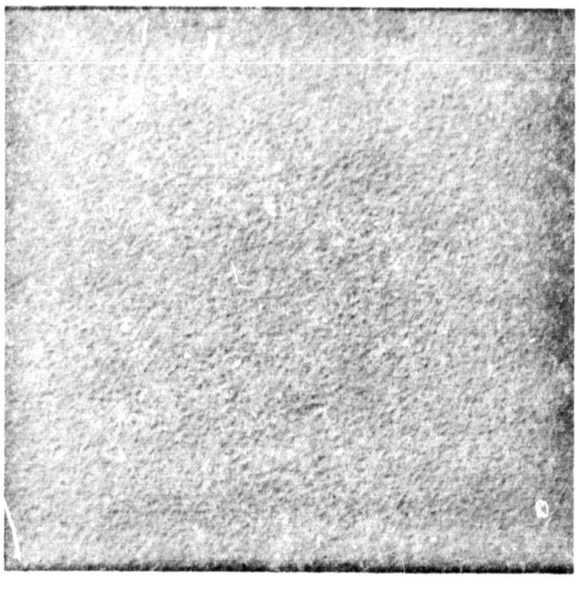

B. Nesa Coating Surface, Electron Microscope Replica, X11,000

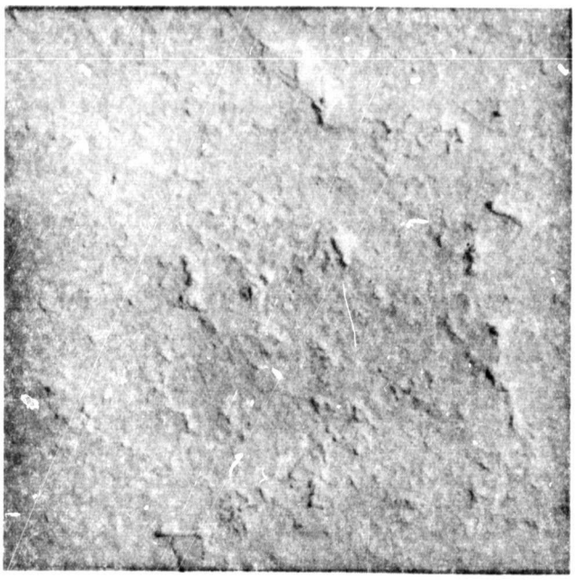

C. Photoconductive Surface, Electron Microscope Replica, X11,000

Figure 12. Phase II, Set 11, Sample 3 Sample Surfaces

Electrical Measurements

Photocurrent vs. light intensity characteristics were measured on selected vidicon face plates by Walter Viehmann, Electronic Materials Section. Aluminum contact areas were vapor-deposited on the photoconductive sulfur-selenium surface and to the underlying conductive tin oxide layer, and pressure contacts were applied to a pair of these contacts. The face plate was kept in a darkened enclosure and it was illuminated through the quartz side of the face plate. The light intensity was variable by inserting neutral density filters into the light path, resulting in measuring different photoconductive currents.

Certain face plates were selected for the electrical measurements. A choice was made of samples having a wide disparity in sulfur-selenium ratio, photoconductor thickness, and grain size.

The effect of the presence of grain boundaries was quickly evident. In these two samples

Phase I Set 5 Plate 2	4240 Å thick, medium grain size
Phase I Set 5 Plate 3	6350 Å thick, large grain size

no measurements were possible because of a short-circuit from the vapor-deposited aluminum contact to the tin oxide conductive layer under the photoconductor. As is apparent from the previous scanning electron microscope pictur[illegible] the grain boundaries extend deeply below the surface to provide a path for the [illegible]or-deposited aluminum.

The effect of having a heavy photoconductive layer was also noted. These two samples

Phase II Set 6 Plate 1	11,260 Å thick, tiny grains
Phase II Set 7 Plate 1	11,920 Å thick, large grains

were unsatisfactory; they were insensitive to light and apparently had no storage capability.

The variation of photocurrent with light intensity is presented for four typical face plates in Figure 13. These include

I.	Phase II Set 4 Plate 1	5,680 Å thick, tiny grains
II.	Phase II Set 2 Plate 1	7,380 Å thick, tiny grains
III.	Phase II Set 6 Plate 1	11,260 Å thick, tiny grains
IV.	Phase II Set 7 Plate 1	11,920 Å thick, large grains

The photocurrent vs. light intensity for III and IV are significantly poorer than for I and II producing a very low current for the 100% light and also having no observable storage. The samples I and II have very similar curves except at the low light levels. It was also observed that this is an indication of the storage capability; after 2 to 3 seconds in the dark after charging, no charge was left on II whereas about 30% of the initial charge was still left on I after 60 seconds. All of these measurements were conducted in air.

The one remaining measured variable between samples I and II is the sulfur-selenium ratio, with sample I having a ratio of 0.268 and sample II having a ratio of 0.278. The difference between a ratio 0.268 and 0.278 may or may not be significant. An attempt to determine the dark current value for a face plate having a sulfur-selenium ratio of 0.372 was not successful because the value was less than 10^{-10} amps and was approaching that of the noise level. However, the indications are that a sulfur-selenium ratio of approximately 0.270 as for sample I is a desireable ratio.

ACKNOWLEDGMENTS

The electron probe results were obtained by Lawrence Kobren and the transmittance and reflectance patterns by Ronald Hunkeler, members of the Ceramics Section.

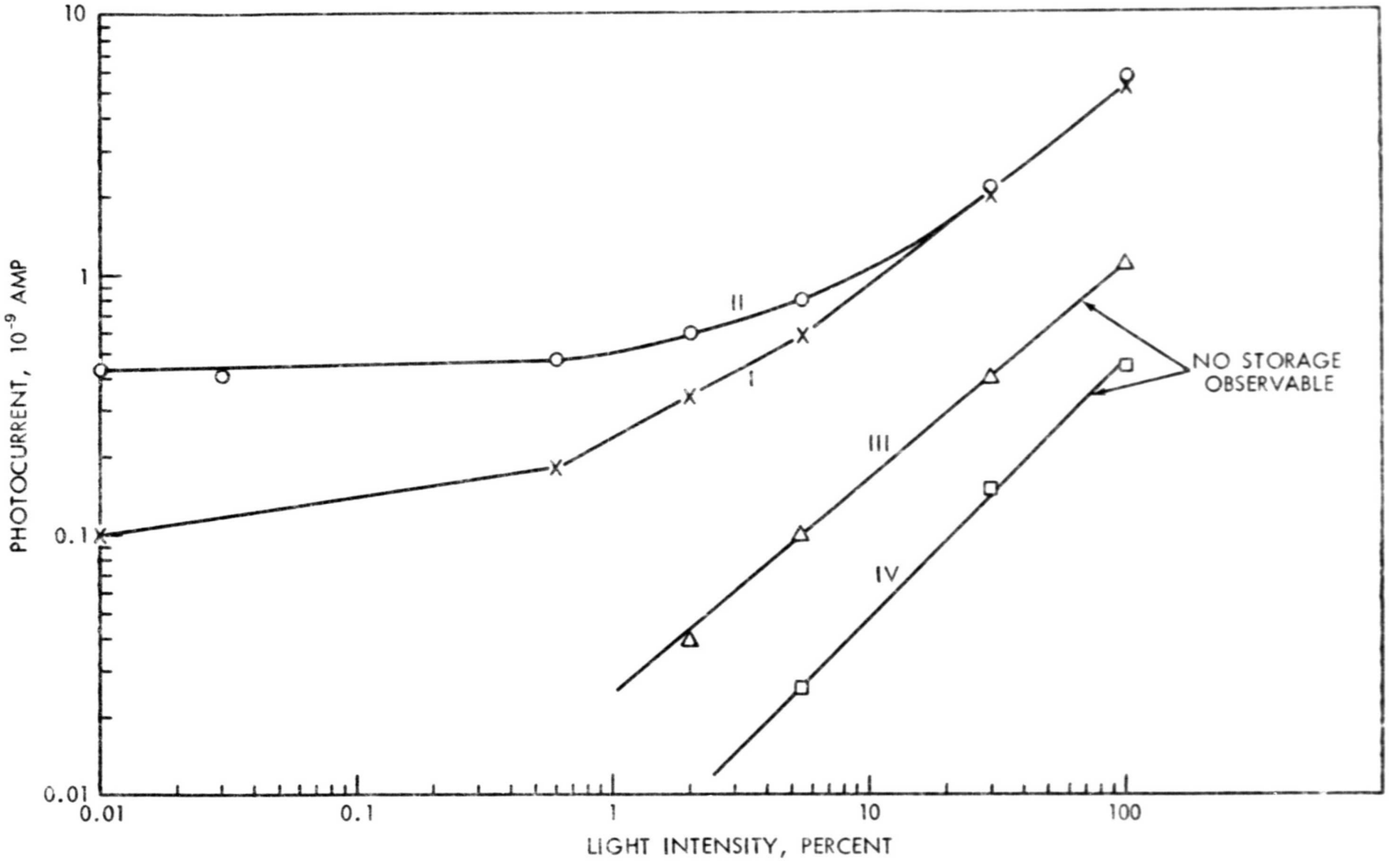

Figure 13. Electrical Characteristics of Face Plates

ADDENDUM

On June 19, 1969 patent 3,450,564, assigned to General Electrodynamics Corporation, was issued. The invention by Stanley A. Bynum was first applied for on June 28, 1965 and a continuation was filed on April 1, 1968. The patent involves melting a mixture of selenium plus 1/2% to 20% by weight of sulfur, evaporating the mixture onto a substrate, then heating the evaporated film to about 100°C to convert the film to a less transparent but still amorphous form of selenium having a darker red color than the ordinary red amorphous selenium. The resultant darker red amorphous form has "higher photosensitivity, a dark resistivity of at least about 10^{10} ohm-cm., and high resistance to conversion to a gray crystalline form at temperatures up to about 70°C."